

# Domes, Rings, Ridges, and Polygons: Characteristics of Microbialites from Utah's Great Salt Lake

Michael D. Vanden Berg

Utah Geological Survey, Salt Lake City, Utah  
michaelvandenber@utah.gov, 801-538-5419

## INTRODUCTION

Two recent events have put Great Salt Lake (GSL) in northern Utah at the forefront of microbialite research. First, massive oil accumulations were discovered in the mid-2000s in offshore South Atlantic “pre-salt” deposits of Cretaceous lacustrine carbonates, including purported microbialites. Petroleum geologists working the pre-salt reservoirs fanned the globe looking for analogs to better understand lacustrine systems and the unique highly permeable and porous deposits called microbialites. At about the same time, GSL experienced record low levels not seen since the early 1960s, exposing one of the world's largest Holocene accumulations of lacustrine microbialites. As a result, GSL quickly became a must visit locale for petroleum geologists.

In light of this new international interest, researchers have sought to better understand GSL microbialites their age, formation mechanisms, distribution, and relationship to other lake facies. This paper provides an introduction to the basic morphology of these unique structures and how local environmental conditions, as well as periods of exposure and erosion, contribute to growth location, grouping, shape, size, orientation, and internal structure. Several other research groups are exploring other important aspects including mineral precipitation mechanisms (Bouton et al., 2016; Pace et al., 2016), biogeochemistry/microbiology (Lindsay et al., 2016; Baxter, 2018), and possible age of formation and paleoenvironmental record (Newell et al., 2017; Vennin et al., 2019).

## BACKGROUND

GSL is the remnant of Pleistocene (32-12 ka) Lake Bonneville, which covered 52,000 km<sup>2</sup> of northwestern Utah as well as small parts of northeastern Nevada and southeastern Idaho (Gwynn, 1996). Lake Bonneville first retreated due to a catastrophic flood into the Snake River Plain, but then the changing climate (warmer and drier) further reduced its size, leaving behind present-day, hypersaline GSL.

GSL averages 121 km long and 56 km wide, covering 4100 km<sup>2</sup>, and fills the lowest depression in the terminal Bonneville basin (Fig. 1). The volume of water in the lake varies both annually and seasonally depending on catchment precipitation, whereas water loss is primarily due

to evaporation (~3600 hm<sup>3</sup> per year; Gwynn, 1996). GSL surface elevation has fluctuated nearly 6 m over recorded history (since 1847), with a long-term elevation average of ~1280 m (4200 ft) above mean sea level (Fig. 1, inset). GSL is shallow, maximum depth is ~10 m, and has broad low-gradient shorelines (Fig. 1). These shallow nearshore areas are favorable for microbialite formation but are also subject to exposure as lake levels fluctuate.

In the late 1950s, a gravel-filled railroad causeway was constructed across the lake, isolating the north arm from the rest of the lake (Fig. 1). With none of the four major rivers entering the north arm, the salinity climbed to 24-26% (near halite saturation), whereas the salinity of the south arm is 12-14% and probably more representative of Holocene conditions.

Post-Bonneville Holocene lake level fluctuations are poorly understood (Murchison, 1989), but measured lake level records reach back to 1847 (Fig. 1, inset). With some exceptions, it is generally assumed that Holocene (since ~12 ka) and historic lake level fluctuations were similar in magnitude and frequency, notwithstanding the anthropogenic influences that have contributed to the more recent low lake level (Wurtsbaugh, 2016). One exception may be the warm/dry period during the mid-Holocene Climatic Optimum (~8-6 ka), in which the lake might have dropped to 6 m below the historic average (Murchison, 1989; Steponaitis, 2015).

Two previous decade long periods where lake levels receded below 1278.6 m (4195 ft), exposing the GSL microbialites, were initiated in 1935 and 1960 (Fig. 1, inset). Eardley (1938) provided the earliest definitive work on “algal bioherms” and associated deposits, including the importance of bacteria in their formation. Carozzi (1962) and Post (1980) described GSL “algal biostromes” and the precipitation of calcium carbonate by “blue-green algae,” and Halley (1976) investigated the textural variations within GSL “algal mounds.” As a result of the more recent low lake levels, Lindsay et al. (2016) researched the living microbial communities and their abilities to survive in a hypersaline environment, while Baskin (2014) attempted to characterize the lake-wide distribution and depth of GSL microbial “bioherms.” In addition, Chidsey et al. (2015) and Della

Porta (2015) looked more closely at GSL microbialite characteristics and facies associations. Moreover, a possible older generation (~12 ka) of GSL microbialites are present at higher elevations (1281.7-1284.7 m, 4205-4215 ft; not further discussed). Examples include the well-lithified microbialites, with associated multi-meter-scale travertine mounds, near Lakeside (Homewood et al., 2018) and the heavily eroded remnants of microbialites near Rozel Point (Chidsey et al., 2015).

## CHARACTERISTICS OF GSL MICROBIALITES

### Basic Microbialite Characteristics

The spatial distribution of GSL microbialites, and their relationship to lake bathymetry (Baskin and Allen, 2005; Baskin and Turner, 2006), was estimated based on examination of Google Earth imagery as well as limited field mapping (Fig. 1). These boundaries will continue to be refined through additional field work. The morphology of GSL microbialites varies according to location. In low-energy areas, like sheltered Bridger Bay at the northern tip of Antelope Island, the microbialites range from nearshore, low-relief and poorly lithified circular “mats” (collapsed domes?, see below) (Fig. 2A), to deeper water, poorly lithified but higher relief domes, all averaging ~15-91 cm in diameter. In contrast, microbialites in higher energy areas, like the east side of Stansbury Island, can be much larger (including the largest domal structure found to date at ~3 m in diameter and ~2 m tall) and better lithified (Fig. 2B). Low-relief elongate microbialites are also present on the west side of the lake (Fig. 2B, structures surrounding the large dome). Images from several unmanned aerial vehicle (UAV) transects were used to better characterize GSL microbialite morphology by lake location and shoreline proximity. For example, figure 2C shows unique linear trends, perpendicular to wave direction, near the northern tip of Antelope Island. This high-resolution imagery shows that

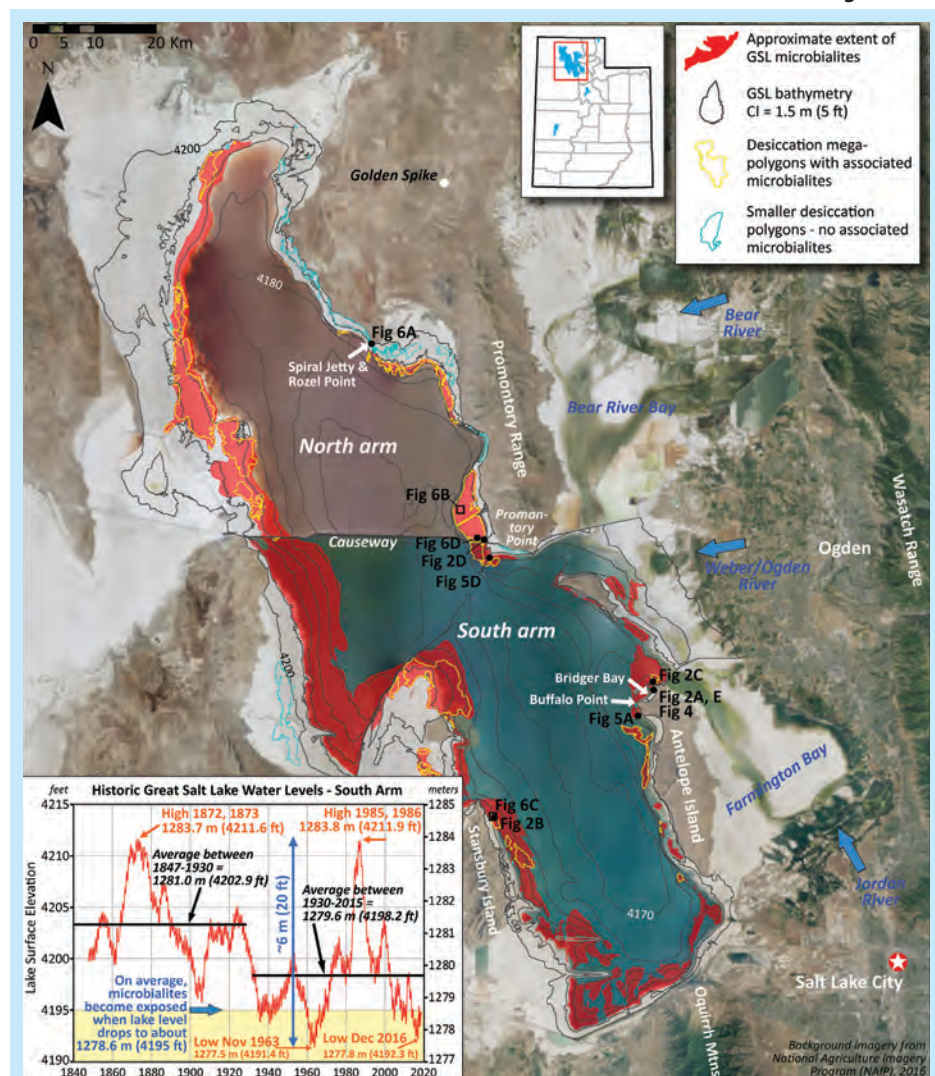


Figure 1: Aerial image of GSL and surrounding highlands from 2016 displaying estimated microbialite extent and areas with shrinkage polygons. Locations of photographs from subsequent figures are shown; lake bathymetry is from Baskin and Allen (2005) and Baskin and Turner (2006). The inset graph shows elevation of GSL through recorded history, 1847-2018 (USGS, 2019).

GSL microbialites, at least in Bridger Bay, are densest near an elevation of 1277.7 m (4192 ft). Compared to an average historic lake level of ~1279.6-1280.2 m (4198-4200 ft), this suggests that GSL microbialites prefer water depths of 1.8-2.4 m.

The microbialites in GSL are found in both the north and south arms (Fig. 1). Submerged microbialites in the south arm are covered with a green-brown, pustular microbial mat that is absent on the microbialites in the ultra-hypersaline north arm. During low lake levels, exposed north arm microbialites are covered with and encased in halite, as well as a thin crust of calcium carbonate (Fig. 2D). Based on analysis

of microbes collected from the surface of GSL microbialites, Lindsay et al. (2016) concluded that the microbial communities found in the north and south arms are distinct. Significantly, the south arm structures contain more photoautotrophic taxa (the green-brown mats), which could drive carbonate precipitation, than are found on north arm microbialites. These observations suggest that all GSL microbialites were forming prior to causeway construction, in lake-wide chemical conditions similar to the present-day south arm. If the microbialites are still “growing” today, growth is limited to the south arm, and north arm microbialites are simply relict structures.

# The Sedimentary Record

GSL microbialites are difficult to place into the traditional microbialite classification scheme of Riding (2000). Their internal composition is mostly structureless (leiolite?) (Fig. 2E), but some are composed of thick (7.6–15.2 cm), poorly defined layers (stromatolites?), but are definitely not finely laminated. Detailed microfacies analysis of high-resolution photomicrographs (Fig. 3A) shows that these structures are mostly composed of captured grains (~40%, mostly carbonate grains [e.g., ooids and pellets]) but sometimes up to 10% lithics (Fig. 3B–C) and pore space (~30%, mostly interparticle pores and constructional vugs), with only ~30% of the structure composed of fibrous aragonitic microbial “clots” (thrombolite?) (Fig. 3A–B, 3D). The clots are the best indication of direct calcium carbonate precipitation from microbes as they mirror the microscopic box-work-like structure of the cyanobacteria in the living microbial mats (Fig. 3D).

## Microbialite Rings

In nearshore areas of GSL, which have historically been under water but are exposed at low lake levels, the microbialites display a ring-shaped structure. These patterns are particularly noticeable on the northern shore of Bridger Bay, Antelope Island, and range in size from 0.5 m to 2 m in diameter. Several UAV transects show a clear offshore to nearshore transition of fully formed domes (at elevations <1277.6 m, <4191.5 ft), to collapsed domes (<1278.0 m, <4193.0 ft), to ring structures (<1278.9 m, <4196.0 ft) (Fig. 4A).

These microbialite rings are interpreted as a result of exposure and erosion of what were once more typical, fully-submerged domal structures, as opposed to primary constructs (Fig. 4A–B). First, microbialite domes of various sizes formed in several feet of water in nearshore environments and, when submerged, are covered with a microbial mat (Fig. 4B). However, in some cases (like in Bridger Bay), the domal structure is not solid and consists

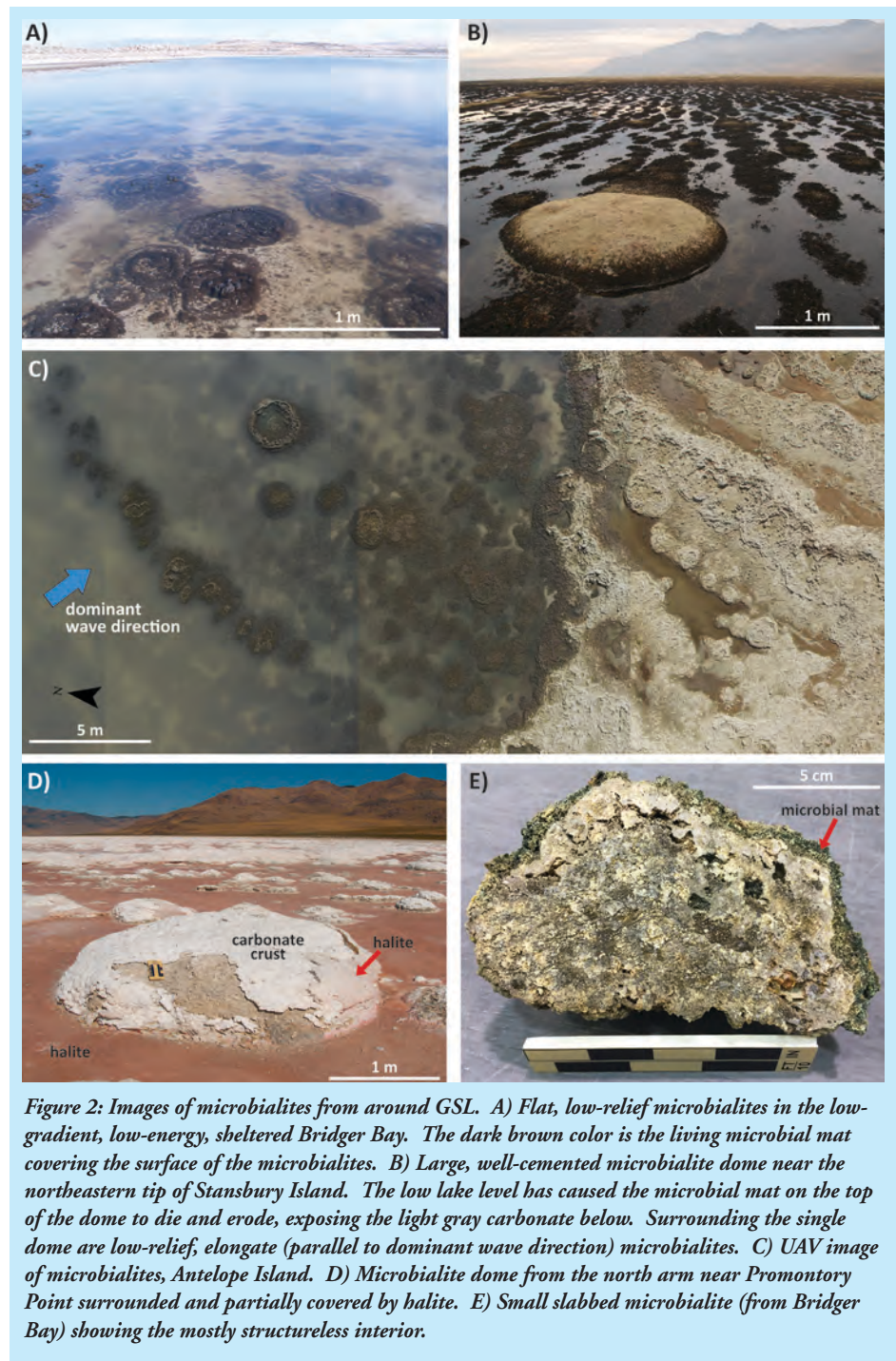


**Figure 2: Images of microbialites from around GSL.** A) Flat, low-relief microbialites in the low-gradient, low-energy, sheltered Bridger Bay. The dark brown color is the living microbial mat covering the surface of the microbialites. B) Large, well-cemented microbialite dome near the northeastern tip of Stansbury Island. The low lake level has caused the microbial mat on the top of the dome to die and erode, exposing the light gray carbonate below. Surrounding the single dome are low-relief, elongate (parallel to dominant wave direction) microbialites. C) UAV image of microbialites, Antelope Island. D) Microbialite dome from the north arm near Promontory Point surrounded and partially covered by halite. E) Small slabbed microbialite (from Bridger Bay) showing the mostly structureless interior.

of a poorly lithified outer shell, 5–15 cm thick, with mostly unconsolidated clay and ooids in the interior. Next, as lake level falls and the water table drops, there is a corresponding decrease in pore pressure. The unconsolidated clay and ooids compact and the microbialite dome collapses, leaving behind a raised outer ring. With continued exposure, the microbial mat dies and erodes, leaving behind only the whitish-gray carbonate. With prolonged exposure and continued erosion, possibly aided

by brief periods of inundation or storm action, the central collapsed part of the microbialite further disintegrates. Continued wave action washes out the broken material, leaving behind only the outer ring. If lake level rises again for an extended period (like from the 1960s to the early 2000s), the eroded ring structure can be recolonized by microbes and a new microbial mat can form. An alternate hypothesis is that the rings could be early primary structures where growth in the central

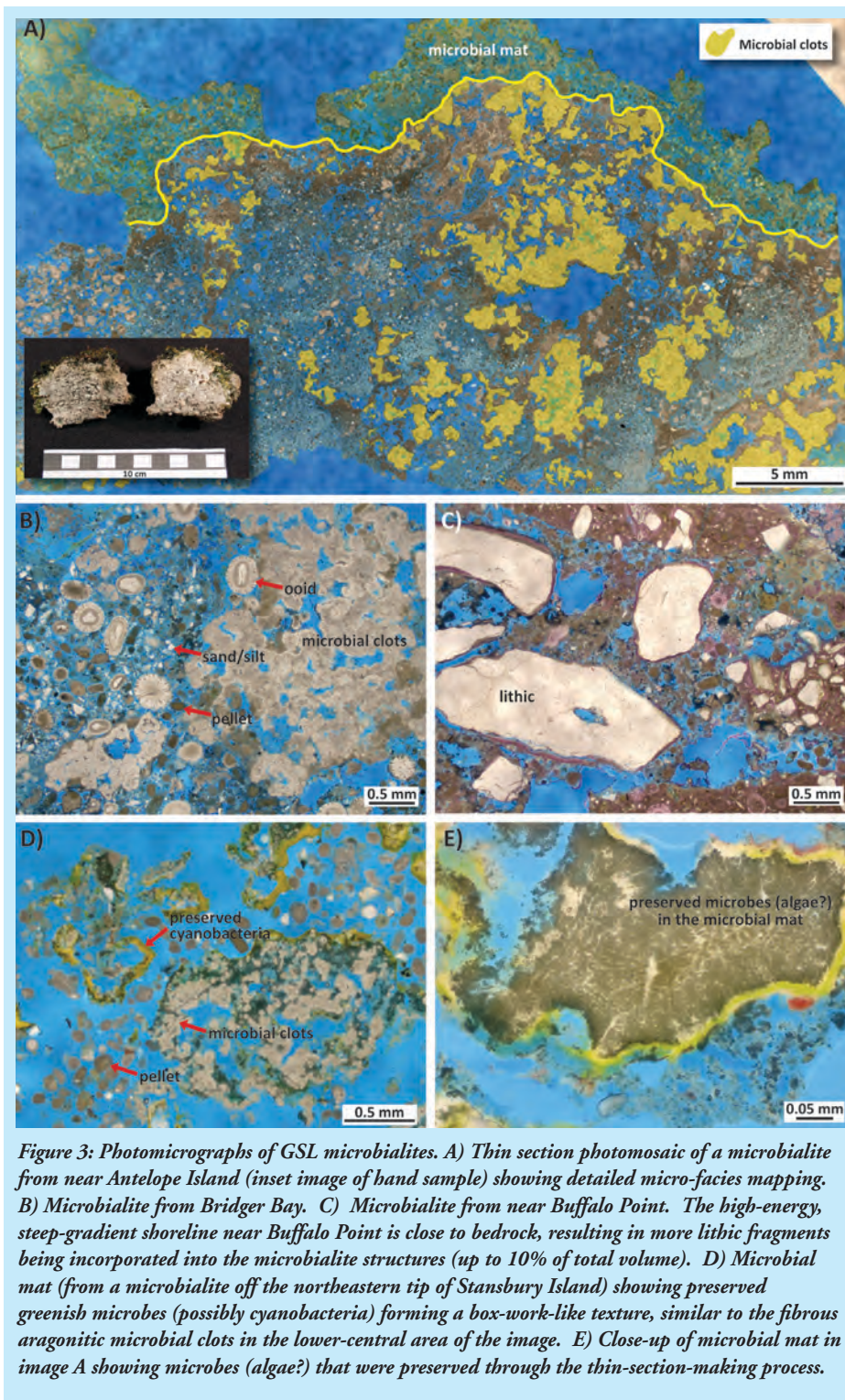


**Figure 3: Photomicrographs of GSL microbialites.** A) Thin section photomosaic of a microbialite from near Antelope Island (inset image of hand sample) showing detailed micro-facies mapping. B) Microbialite from Bridger Bay. C) Microbialite from near Buffalo Point. The high-energy, steep-gradient shoreline near Buffalo Point is close to bedrock, resulting in more lithic fragments being incorporated into the microbialite structures (up to 10% of total volume). D) Microbial mat (from a microbialite off the northeastern tip of Stansbury Island) showing preserved greenish microbes (possibly cyanobacteria) forming a box-work-like texture, similar to the fibrous aragonitic microbial clots in the lower-central area of the image. E) Close-up of microbial mat in image A showing microbes (algae?) that were preserved through the thin-section-making process.

portion of the microbialite is inhibited due to nearshore erosional processes.

### Microbialite Ridges

In a few areas around GSL, microbial mats form small (10-15 cm wide, 5-10 cm tall), linear ridges that are continuous for several meters (Fig. 5A-C). These structures are typically parallel to shore and perpendicular

to wave action. The most probable interpretation for the ridge formation is related to the lithification of wave ripples on an ooid sand bar. In specific areas, wave ripples formed in nearshore areas adjacent and slightly south of rocky points of land (e.g., southwestern tip of Buffalo Point on Antelope Island and the southern, lakeward tip of Promontory Point). At some point,

isopachous aragonite cement developed (Fig. 5D), as well as exposure-related meniscus cements, which partially lithified the ooid sand preserving the ripple shape (Fig. 5E). After a rise in lake level and continued wave action, the troughs of the preserved ripples filled with unconsolidated ooid sand, but the crests of the ripples remained as slightly elevated hard substrates. With continued inundation, microbial mats formed on the crests of the preserved ripples (Fig. 5A-C). Similar to the microbialite rings, when the ridges are exposed, the microbial mat erodes off leaving behind the lithified ooid sand ridges (Fig. 5D), which could be re-colonized if lake levels rise again.

### Polygonal Structures and Groundwater

Shrinkage polygons are common along the shallow shores of saline/playa lakes (Neal et al., 1968). These structures were first recognized around GSL by Currey (1980) and later referenced by Bouton et al. (2016) and Janecke and Evans (2017). In GSL, two types of polygons were identified: 1) smaller polygons that form closer to shore at slightly higher elevations, and 2) larger, mega-polygons that formed farther out on the shallow shelf at slightly lower elevations. With the increased resolution of aerial imagery (e.g., Google Earth), combined with historic low lake levels, these unique structures are easily observed and mapped around the lake (Fig. 1).

Small-scale shrinkage polygons can be observed near Rozel Point in the north arm (Fig. 6A). On average these features are 4-9 m in diameter and form on the exposed lake bed closer to the high-water line, between ~1278.3-1279.9 m (4194-4199 ft) in elevation. The surface of the lake bed is mostly composed of ooid sand and mud, underlain by clay. The polygons form when lake level retreats and exposure results in desiccation of the nearshore sediments. The cracked perimeter of the polygons is filled by upwelling clay, possibly aided by groundwater movement (Fig. 6A, inset). The

## The Sedimentary Record

clay forms raised ridges making the polygons easily identified on aerial imagery. These smaller polygons are interpreted as “recent” ephemeral features that come and go with seasonal changes in lake level and are not generally associated with microbialites.

The large-scale polygons observed on the shallow lake margins, slightly deeper than the smaller polygons, are truly remarkable, not only for their size, but also their direct association with GSL microbialites (Fig. 6B-D). On average, these mega-polygons are 30-75 m in diameter and cover ~145 km<sup>2</sup> of the offshore margins around GSL (Fig. 1). The perimeters of the mega-polygons became preferred locations for extensive microbialite formation (Fig. 6C-D). Using the smaller polygons as an analog, it is assumed that the perimeters were areas of slightly higher topography due to upwardly injected clay, which could have created a preferred location for microbialite growth. In addition, the upwelling around the perimeter suggests a pathway for groundwater (Fig. 6E). Calcium-rich groundwater could have increased the ability of microbes to mediate the precipitation of calcium carbonate, leading to extensive microbialite formation. In fact, these polygon-associated microbialites are more cemented/lithified, and hence less likely to collapse, compared to microbialites in other locations.

The timing of mega-polygon formation is unknown, but if the polygons formed during a period of exposure, their formation timing can be constrained based on their elevation compared to lake level records. The lowest elevation with mega-polygon structures is ~1275.6 m (4185 ft), the last time lake level is hypothesized to have receded below this level was during the mid-Holocene Climatic Optimum (~8-6 ka; Murchison, 1989; Steponaitis, 2015). As with the smaller polygons, a subsequent rise in lake level would rapidly degrade and/or destroy the polygonal structures. Thus, the excellent preservation of the mega-polygons could suggest that the

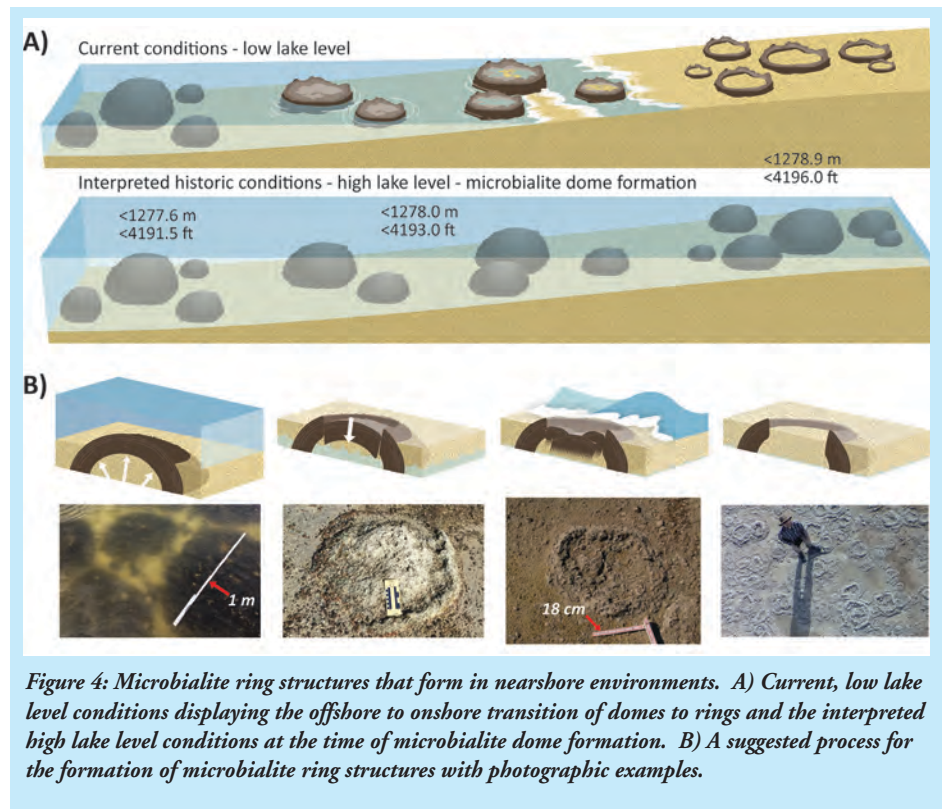


*Figure 4: Microbialite ring structures that form in nearshore environments. A) Current, low lake level conditions displaying the offshore to onshore transition of domes to rings and the interpreted high lake level conditions at the time of microbialite dome formation. B) A suggested process for the formation of microbialite ring structures with photographic examples.*

rimming GSL microbialites formed rather rapidly during a large-scale lake level transgression, preserving the polygonal shape before the sediments could be reworked. This also suggests that these microbialites are relatively old (~6 ka) and not “modern” like has been suggested.

These interpretations suggest an important link between microbialites and groundwater within GSL, similar to findings in the ancient lacustrine rock record, particularly the Green River Formation (e.g., Awramik and Buchheim, 2015). The microbialites on the perimeters of the polygons are often large, well-formed, and more lithified than microbialites in areas like Bridger Bay, possibly due to the availability of calcium-rich groundwater. In some cases, pathways in the interiors of the domal microbialites are lined with a dense, finely laminated travertine-like carbonate, an indication that groundwater is flowing through these structures. Further research could clarify the possibly underappreciated role groundwater contributes to the formation of GSL microbialites.

## SUMMARY

Recent oil discoveries in South Atlantic pre-salt lacustrine reservoirs, as well as historic low lake levels of GSL, have greatly renewed and heightened interest in the lake’s microbialite population. Researchers are beginning to recognize that these structures are unique compared to other global ancient and recent microbialite examples, but similarities also exist. GSL microbialites do not easily fit into the recognized microbialite naming convention, given that they are mostly structureless and are made up of dominantly loosely cemented carbonate grains and debris, display significant porosity, and contain only minor accumulations of microbial clots. The main driver of GSL microbialite morphology is mostly related to local environmental and lake conditions. Periods of exposure and erosion also play a large role in their morphology. In addition, the possible importance of groundwater on the formation of GSL microbialites and their growth location is becoming more apparent. Several questions still remain unanswered and should be the focus of future studies, including: 1) What is the precise age for

**ACKNOWLEDGEMENTS**

David Eby and Thomas Chidsey made significant contributions to this project. This research also benefited greatly from discussions and field excursions with S. Awramik, B. Baxter, E. Boyd, P. Buchheim, C. Frantz, M. Lindsey, and D. Newell. B. Pratt and J. Bishop provided extensive reviews that greatly improved this manuscript, as well as suggestions by the editor, L. Birgenheier.

**REFERENCES**

- AWRAMIK, S.M. AND BUCHHEIM, H.P., 2015, Giant stromatolites of the Eocene Green River Formation (Colorado, USA): *Geology* 43 (8), 691-694.
- BASKIN, R.L. AND ALLEN, D.V., 2005, Bathymetric map of the south part of Great Salt Lake, Utah: USGS Scientific Investigations Map 2894.
- BASKIN, R.L. AND TURNER, J., 2006, Bathymetric map of the north part of Great Salt Lake, Utah: USGS Scientific Investigations Map 2006-2954.
- BASKIN, R.L., 2014, Occurrence and spatial distribution of microbial bioherms in Great Salt Lake, Utah: PhD dissertation, Dept. of Geography, University of Utah, 190 p.
- BAXTER, B.K., 2018, Great Salt Lake microbiology: a historical perspective: *International Microbiology* 21, 79-95.
- BOUTON, A., VENNIN, E., BOULLE, J., PACE, A., BOURILLOT, R., THOMAZO, C., BRAYARD, A., DÉSAUBLIAUX, G., GOSLAR, T., YOKOYAMA, Y., DUPRAZ, C., AND VISSCHER, P.T., 2016, Linking the distribution of microbial deposits from the Great Salt Lake (Utah, USA) to tectonic and climatic processes: *Biogeosciences* 13, 5511-5526.
- CAROZZI, A.V., 1962, Observations on algal biostromes in the Great Salt Lake, Utah: *The Journal of Geology* 70 (2), 246-252.
- CHIDSEY, T.C., JR., VANDEN BERG, M.D., AND EBY, D.E., 2015, Petrography and characterization of microbial carbonates and associated facies from modern Great Salt Lake and Uinta Basin's Eocene Green River Formation in Utah, USA, in: Bosence, D.W.J., et al. (Eds.), *Microbial Carbonates in Space and Time: Implications for Global Exploration and Production*: Geological Society, London, Special Publications 418.
- CURREY, D.R., 1980, Coastal geomorphology of Great Salt Lake and vicinity, in: Gwynn, J.W. (Ed.), *Great Salt Lake A Scientific, Historical and Economic Overview*: Utah Geological and Mineral Survey Bulletin 116.
- DELLA PORTA, G., 2015, Carbonate build-ups in lacustrine, hydrothermal and fluvial settings: comparing depositional geometry, fabric and geochemical signature, in: Bosence, D.W.J., et al. (Eds.), *Microbial Carbonates in Space and Time: Implications for Global Exploration and Production*: Geological Society, London, Special Publications 418.
- EARDLEY, A.J., 1938, Sediments of the Great Salt Lake: *AAPG Bulletin* 22, 1305-1411.

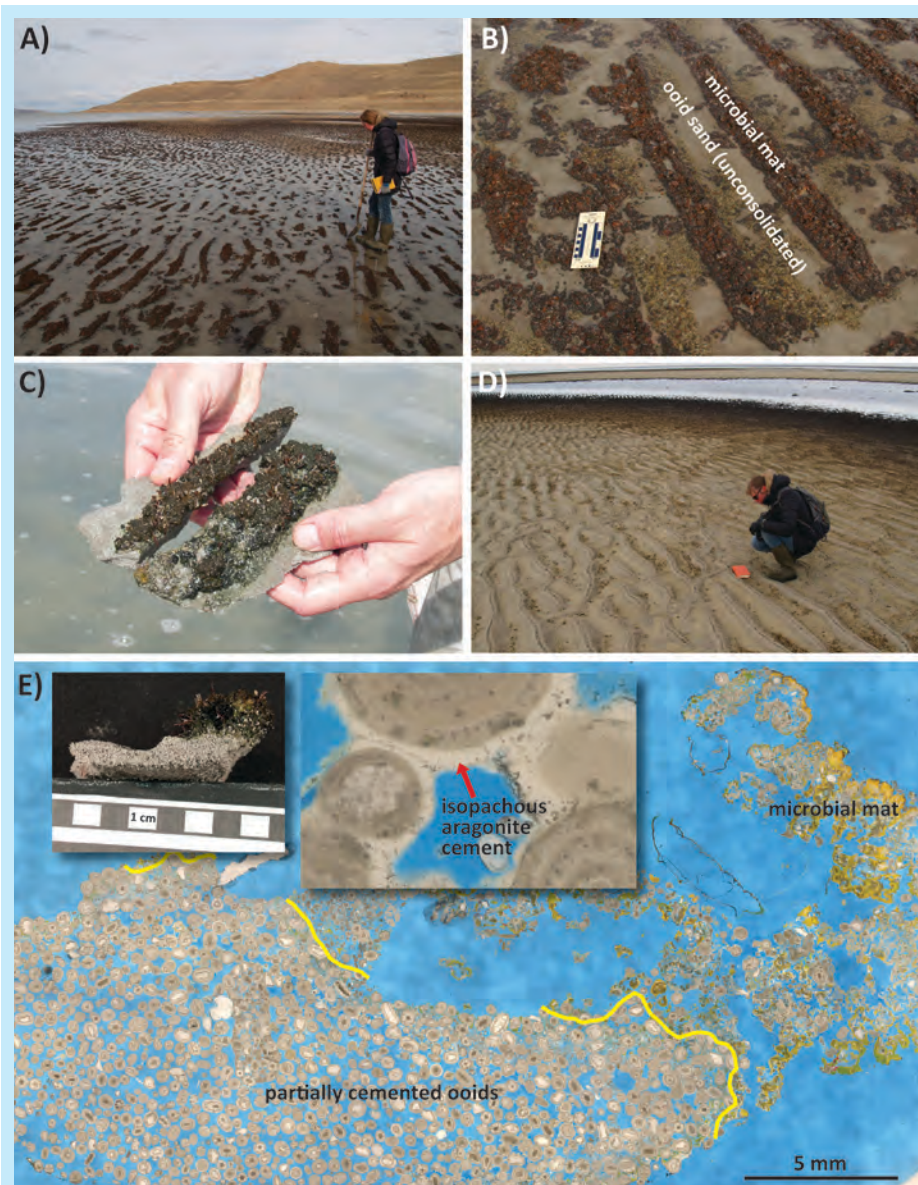


**Figure 5:** Microbialite ridge structures that form on the crests of cemented wave ripples. **A)** Ridges off the southwestern tip of Buffalo Point. The ridges are oriented north-south and are mostly perpendicular to wave direction. **B)** Close-up of ridges near Buffalo Point. **C)** Cemented ooid sand wave ripple with microbial mat covering the ripple crest. **D)** Ridges exposed near the southwestern tip of Promontory Point; the microbial mat has eroded, exposing the underlying cemented ooids. **E)** Photomicrograph of the cemented ooid sand ripple with microbial mat (inset image of hand sample). The close-up inset image shows isopachous cement around the ooids.

GSL microbialite formation?

2) Has there been more than one period of development? 3) Does the microbe community that currently inhabits the microbial mats mediate the precipitation of new calcium carbonate or are the microbes simply taking advantage of hard relict substrates? 4) Presently the lake water is depleted in calcium relative to other major ions; at other points in the lake's history, maybe during periods of high run-off (transgressions), could the same

microbes that live in the lake today "build" these structures?

With lake levels projected to remain low, researchers will continue to have unprecedented access to these remarkable structures. Further research will not only provide a better understanding of lacustrine hydrocarbon reservoirs but will also provide insights into the evolution of GSL geomicrobiology and how it relates to the rest of this important ecosystem.

# The Sedimentary Record

- GWYNN, J.W., 1996, Commonly asked questions about Utah's Great Salt Lake and ancient Lake Bonneville: UGS Public Information Series 39, 21 p.
- HALLEY, R.B., 1976, Textural variation within Great Salt Lake algal mounds, in: Walter, M.R. (Ed.), *Developments in Sedimentology*, Elsevier, 20, 435-445.
- HOMWOOD, P.W., METTRAUX, M., VANDEN BERG, M.D., FOUBERT, A., AND SCHAEGIS, J.C., 2018, Presalt reservoir analogs: Lacustrine microbialites fed by shore zone hot springs, Lakeside UT: AAPG Datapages Search and Discovery.
- JANECKE, S.U. AND EVANS, J.P., 2017, Revised structure and correlation of the Great Salt Lake, North Promontory, Rozel and Hansel Valley fault zones revealed by 2015-2016 low stand of Great Salt Lake, in: Lund, W.R., et al. (Eds.), *Geology and Resources of the Wasatch: Back to Front: Utah Geological Association* 46, 295-318.
- LINDSAY, M.R., ANDERSON, C., FOX, N., SCOFIELD, G., ALLEN, J., ANDERSON, E., BUETER, L., POUDEL, S., SUTHERLAND, K., MUNSON MCGEE, J.H., VAN NOSTRAND, J.D., ZHOU, J., SPEAR, J.R., BAXTER, B.K., LAGESON, D.R., AND BOYD, E.S., 2016, Microbialite response to an anthropogenic salinity gradient in Great Salt Lake, Utah: *Geobiology* 15, 131-145.
- MURCHISON, S.B., 1989, Fluctuation history of Great Salt Lake, Utah, during the last 13,000 years: PhD dissertation: Dept. of Geography, University of Utah, 137 p.
- NEAL, J.T., LANGER, A.M., AND KERR, P.F., 1968, Giant desiccation polygons of Great Basin playas: *GSA Bulletin* 79, 69-90.
- NEWELL, D.L., JENSEN, J.L., FRANTZ, C.M., AND VANDEN BERG, M.D., 2017, Great Salt Lake (Utah) microbialite  $\delta^{13}\text{C}$ ,  $\delta^{18}\text{O}$ , and  $\delta^{15}\text{N}$  record fluctuations in lake biogeochemistry since the late Pleistocene: *Geochemistry, Geophysics, Geosystems* 18, 3631-3645.
- PACE, A., BOURILLOT, R., BOUTON, A., VENNIN, E., GALAUP, S., BUNDELEVA, I., PATRIER, P., DUPRAZ, C., THOMAZO, C., SANSJOFRE, P., YOKOYAMA, Y., FRANCESCHI, M., ANGUY, Y., PIGOT, L., VIRGONE, A., AND VISSCHER, P., 2016, Microbial and diagenetic steps leading to the mineralization of Great Salt Lake microbialites: *Scientific Reports* 6 (31495), 12 p.
- POST, F.J., 1980, Biology of the north arm, in: Gwynn J.W. (Ed.), *Great Salt Lake A Scientific, Historical and Economic Overview: Utah Geological and Mineral Survey Bulletin* 116, 313-321.
- RIDING, R., 2000, Microbial carbonates: the geological record of calcified bacterial-algal mats and biofilms: *Sedimentology* 47, 179-214.
- STEPONAITIS, E., ANDREWS, A., MCGEE, D., QUADE, J., HSIEH, Y., BROECKER, W.S., SHUMAN, B.N., BURNS, S.J., AND CHENG, H., 2015, Mid-Holocene drying of the U.S. Great Basin recorded in Nevada speleothems: *Quaternary Science Reviews* 127, 1-12.
- USGS, 2019, Great Salt Lake—Lake elevations and elevation changes: <https://ut.water.usgs.gov/greatsaltlake/elevations/>

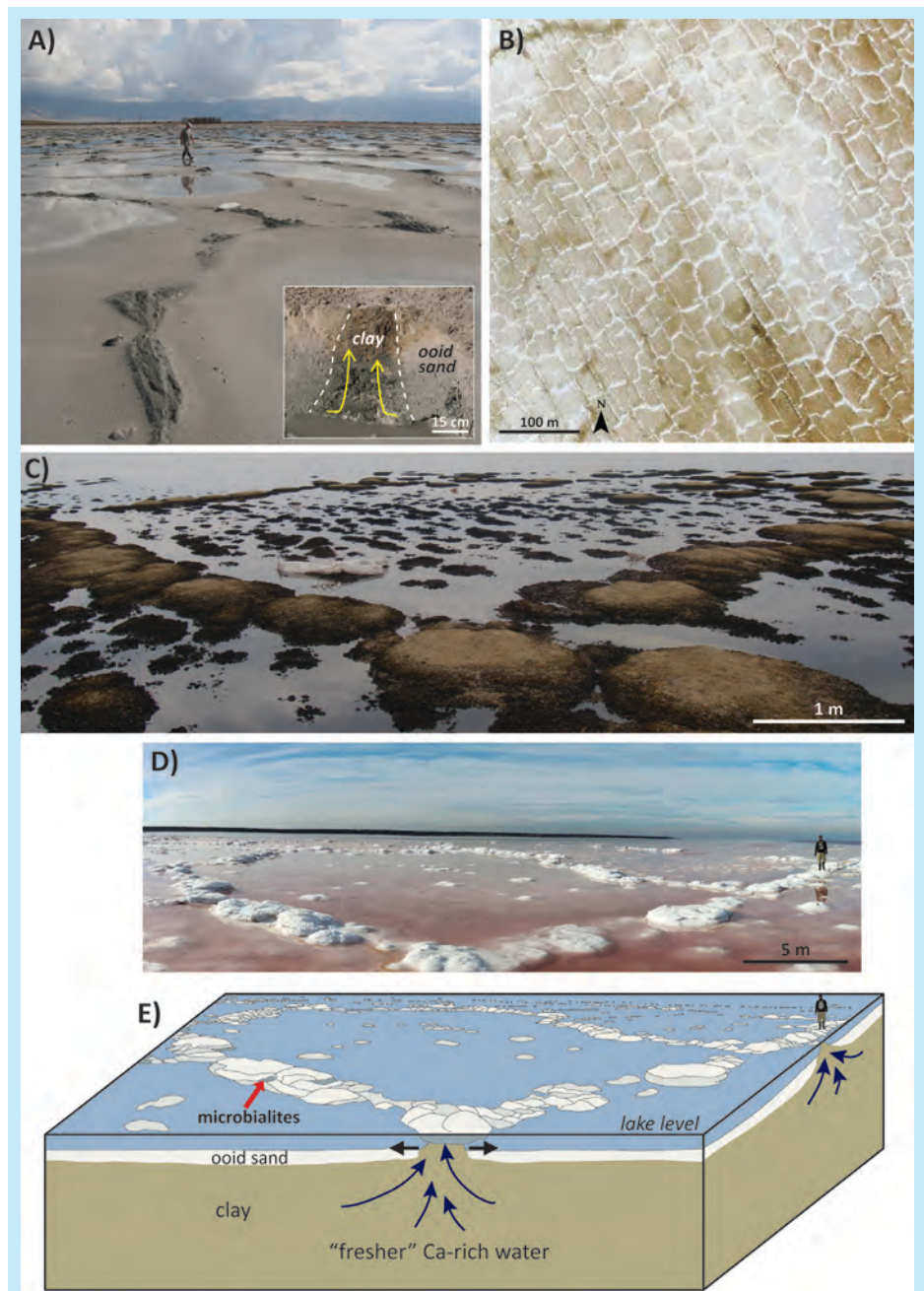


**Figure 6: Images of shrinkage polygons around GSL. A) Small-scale polygons, with upwardly injected clay around the perimeters, Rozel Point (inset, trench through polygon perimeter). B) Google Earth image (August 2014) of mega-polygons near Promontory Point. C) Partially exposed microbialites along the perimeter of a mega-polygon near the northeastern tip of Stansbury Island. D) Mega-polygons and associated microbialites near Promontory Point (whit/pink areas are halite crust). E) Suggested mega-polygon formation mechanism based on photograph in D.**

VENNIN, E., BOUTON, A., BOURILLOT, R., PACE, A., ROCHE, A., BRAYARD, A., THOMAZO, C., VIRGONE, A., GAUCHER, E.C., DESAUBLIAUX, G., AND VISSCHER, P.T., 2019, The lacustrine microbial carbonate factory of the successive Lake Bonneville and Great Salt Lake, Utah, USA: *Sedimentology* 66 (1), 165-204.

WURTSBAUGH, W., MILLER, C., NULL, S., WILCOCK, P., HAHNENBERGER, M., AND HOWE, F., 2016, Impacts of water development on Great Salt Lake and the Wasatch Front: Watershed Sciences Faculty Publications, Paper 875, 9 p.

Accepted March 2019